

Enhanced electrocaloric effect of P(VDF-TrFE)-based nanocomposites with Ca and Sn co-doped BaTiO₃ particles

Melike Tokkan, Mustafa M. Demir, Umut Adem*

Department of Materials Science and Engineering, Izmir Institute of Technology, Urla, 35430, Izmir, Turkey

ARTICLE INFO

Keywords:

Polymer nanocomposites
Nanoparticles
Electrocaloric effect
Ferroelectricity
Poly(vinylidene fluoride-co-trifluoroethylene)
BaTiO₃

ABSTRACT

We report on the enhancement of electrocaloric effect in solution cast polymer nanocomposites based on Poly (vinylidene fluoride-co-trifluoroethylene) [P(VDF-TrFE) 55-45] with Ca and Sn co-substituted BaTiO₃ ceramic fillers (Ba_{0.94}Ca_{0.06}Ti_{0.925}Sn_{0.075}O₃, BCST). Saturated hysteresis loops and normal ferroelectric behaviour of the copolymer-based nanocomposites -as opposed to the relaxor ferroelectric nature of the terpolymer-based ones- allow the utilization of the indirect method to estimate the electrocaloric properties. Both the dielectric constant and electrocaloric temperature change (ΔT) increases as the particle content increases. Maximum adiabatic temperature change was obtained as 6.96 K under 900 kV/cm for the 10 vol % BCST containing polymer composite around the Curie temperature of the copolymer (70 °C). This relatively large electrocaloric strength is slightly lower than those obtained for terpolymer-based nanocomposites.

1. Introduction

Electrocaloric effect is the reversible change in the temperature of the material due to the applied electric field under adiabatic conditions [1,2]. It provides substantial adiabatic temperature change, which can be exploited in electrocaloric cooling applications as an alternative to the conventional vapor compression-based cooling technology. Quite large adiabatic temperature changes have been measured on thin films of ferroelectric polymers, which is already utilized in cooling applications [3,4]. Very recently, it has been shown that it is possible to further optimize the electrocaloric effect in PVDF-based terpolymers by introducing defects without sacrificing the crystallinity, leading to the largest entropy and ΔT changes per applied electric field reported so far [5]. These changes can be further increased by forming composites with ceramic fillers. Ferroelectric ceramics have large electrocaloric strength (electrocaloric temperature change (ΔT) per applied electric field), but also lower dielectric breakdown strength compared to polymers. Ferroelectric polymer-ceramic composites make use of the large dielectric breakdown strength of the polymer matrix and ceramic particles in the composites assist to enhance the electrocaloric effect due to the electric field amplification effect of the ceramic-polymer interfaces [6–13].

Most of the recent studies focus on the composites based on the PVDF-based terpolymers. Due to their relaxor ferroelectric character,

terpolymer-based composites offer a broad temperature range where large ΔT can be maintained. However, the relaxor ferroelectric character also causes depolarization to occur in a broad temperature interval [14]; thus ΔT of the terpolymer is slightly lower than that of the copolymer at the same electric field [15]. In one of the earliest studies, Zhang et al. reported nanocomposites of P(VDF-TrFE-CFE) and Ba_{0.67}Sr_{0.33}TiO₃ nanofillers. They showed that the morphology of the nanofillers significantly influence the electrocaloric response. Fillers with nanowire morphology provided higher dielectric breakdown strength compared to other morphologies including nanoparticles, leading to larger ΔT [8]. Significant increase in ΔT values of the nanocomposites compared to the pristine co- or terpolymer is mainly ascribed to the interface effect. In general, in polymer matrix composites, the interface between the polymer matrix and the reinforcing phases is critical for the mechanical properties [16]. Here, the interface plays between the polymer and the ceramic particle plays a crucial role for the electrical properties by acting as a local electric field concentrator due to the polarization of the ceramic particle under the applied electric field [9]. Phase field simulations also supported this claim [10]. It has been reported that the interface effect can be maximized near the Curie temperature of the ferroelectric ceramic, as the polarization of the filler changes drastically near its Curie temperature [1]. Therefore, adjusting the Curie temperatures of the polymer matrix and the ceramic filler close to each other can increase the interface effect. Unlike the studies of the

* Corresponding author.

E-mail address: umutadem@iyte.edu.tr (U. Adem).

<https://doi.org/10.1016/j.ceramint.2022.09.275>

Received 21 July 2022; Received in revised form 21 September 2022; Accepted 21 September 2022

Available online 24 September 2022

0272-8842/© 2022 Elsevier Ltd and Techna Group S.r.l. All rights reserved.

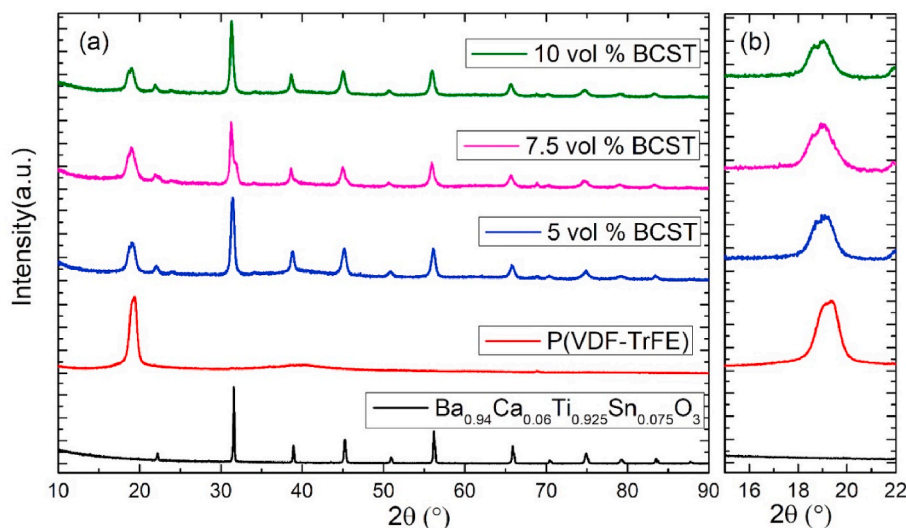


Fig. 1. (a) XRD patterns of BCST, P(VDF-TrFE), 5, 7.5 and 10 vol % BCST containing composites, (b) shows the detailed patterns around the main peak of the copolymer.

nanocomposites based on the terpolymers, there are surprisingly few studies where electrocaloric properties of P(VDF-TrFE) copolymer-based nanocomposites are reported. In general, terpolymer-based nanocomposites necessitate the use of more demanding direct measurement of ΔT , due to their relaxor ferroelectric nature [17]. In contrast, for copolymer compositions with normal ferroelectric behaviour, the use of more convenient indirect method, which is based on Maxwell's equations and measurements of temperature dependent hysteresis loops, is possible [17], but rarely reported. Jiang et al. reported a ΔT of 2.5 °C at 600 kV/cm for P(VDF-TrFE)-52/48-Ba_{0.75}Sr_{0.25}TiO₃ composites however hysteresis loops used to calculate ΔT using the indirect method were not saturated [7]. Same group of authors also reported large negative electrocaloric effect in P(VDF-TrFE)-52/48-BaTiO₃ nanocomposites [18]. While we were in the process of preparing this manuscript, we have also come across a study on a copolymer composite which was fabricated using tape-casting and hot pressing. Remarkably large ΔT of 9.1 K at 500 kV/cm was reported [19].

Here, we report on the electrocaloric effect of nanocomposites of Ca and Sn co-doped BaTiO₃ based ceramic fillers (0, 5, 7.5 and 10 vol %) and P(VDF-TrFE) 55/45 copolymer matrix, which are synthesized using solution casting. Ca and Sn co-doping was used to tune the Curie temperature of the filler close to that of the copolymer and to obtain a relatively broad phase transition of the ceramic filler to increase the temperature range of the interface effect. Owing to the normal ferroelectric behaviour, saturated hysteresis loops and negligible conductivity contribution to the electrical polarization at high temperatures, we demonstrate an accurate estimation of the electrocaloric properties using the indirect method.

2. Experimental

To obtain the ceramic filler powder, (Ba_{0.94}Ca_{0.06})(Sn_{0.0075}Ti_{0.925})O₃ ceramic was synthesized by conventional solid-state reaction. Stoichiometric amounts of BaCO₃ (99.9% Entekno), TiO₂ (99.9% Sigma Aldrich), CaCO₃ (99.999% Sigma Aldrich) and SnO₂ (99.9% Merck) were ground in ethanol with zirconia balls in a Planetary Ball mill (RETSCH PM 100). Resulting powder was calcined at 1200 °C for 4 h. 2 wt % of PVA (as a binder) was added and the powder was pelletized using a hydraulic press (Specac) under 375 MPa. Following the binder burnout at 600 °C for 4 h, pellets were sintered at 1350 °C for 3 h. In order to obtain nanosized powder to be used in the composites, first resulting BCST pellets were ground in an agate mortar. Then the resulting powder was milled using planetary ball milling in ethanol with

yttria stabilized zirconia balls in a 30 ml HDPE Nalgene bottle at 250 rpm for 8 h. The ball to powder weight ratio was 10:1. Final particle size was measured using Dynamic Light Scattering (Zetasizer Nano ZS, Malvern Instruments).

Nanocomposites were synthesized by solution casting. First P(VDF-TrFE) 55/45 (PolyK Technologies, USA) was dissolved in N,N Dimethylformamide (DMF) using a magnetic stirrer (Heidolph Hei-Tec) at 500 rpm for 4 h. Ceramic powder were then added as 5, 7.5 and 10 vol % to the solution and the solution was sonicated for half an hour in an ultrasonic cleaner (ISOLAB) and the final solution was mixed overnight in a magnetic stirrer. Resulting mixture was cast in a Petri dish (diameter: 60 mm, thickness: 10 mm) and DMF was evaporated at 70 °C overnight. The films were heat treated at 135 °C for 3 h.

Phase analysis of the ceramic filler and polymer nanocomposites were done by X-ray diffraction (Both Philips X'pert Pro and Bruker D2 Phaser were used). Microstructure of the samples, the distribution of the ceramic fillers and the thickness of the nanocomposite films were checked using Scanning Electron Microscopy (Philips XL 305 FEG and FEI Quanta 250 FEG). Fourier Transform Infrared Spectroscopy (PerkinElmer) was performed to examine the bond vibrations and functional groups of molecules of thick film polymer, composites and BCST ceramics. Differential Scanning Calorimetry (TA Instruments Q10) was used to carry out thermal analysis of the samples.

For the electrical measurements, square pieces of approximately 15–20 mm width and length were cut, and top and bottom surfaces of the samples were covered with silver paste (RS Components) which was subsequently dried at room temperature for 1 day. Dielectric properties were measured by a Keysight E4980AL Precision LCR meter between 25 and 150 °C and at 0.1, 1, 10 and 100 kHz. Ferroelectric hysteresis loops of the samples were measured using Aixact TF1000 also between 25 and 150 °C. Electrocaloric temperature change (ΔT) of the sample was calculated using the indirect method based on Maxwell's equations (Eq. (1)).

$$\Delta T = -\frac{1}{\rho} \int_{E_1}^{E_2} \frac{T}{C_p} \left(\frac{\partial D}{\partial T} \right)_E dE \quad (1)$$

where D is the dielectric displacement (electrical polarization, P is used interchangeably), E₁, E₂ are initial and final electric fields, C_p is the heat capacity, ρ is the density and T is the temperature. In these calculations, density of the composites was estimated by the rule of mixtures as 1.898, 1.997, 2.096 g/cm³ for 5, 7.5 and 10 vol % BCST containing composites.

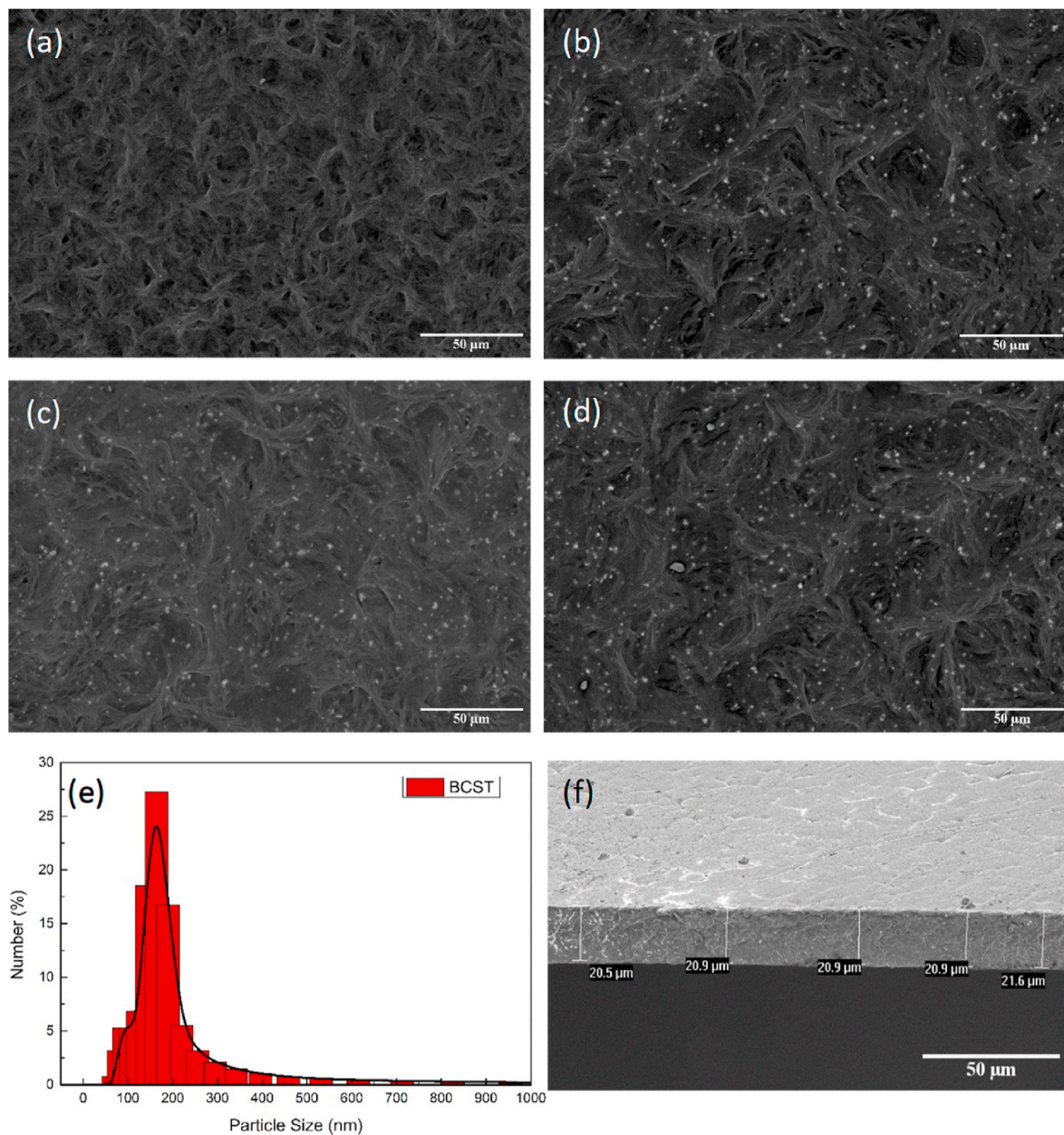


Fig. 2. Back Scattered SEM images of (a) P(VDF-TrFE) 55-45 thick film, (b) 5 vol %, (c) 7.5 vol % and (d), 10 vol % BCST containing composites; (e) size distribution of BCST particles used in the composites, (f) cross-sectional SEM image of the 21 μm thick pristine polymer, representative of all thick films.

The values of $(\partial D/\partial T)_E$ ($(\partial P/\partial T)_E$) were obtained either by fitting $P(T)$ curves using a sixth order polynomial close to T_C between 50 and 80 $^\circ\text{C}$ (applied to the data shown in Fig. 6(a) to obtain smooth ΔT curves), or by using small linear increments using $(\frac{\partial P}{\partial T})_E = \frac{1}{2} * (\frac{P_n - P_{n-1}}{T_n - T_{n-1}} + \frac{P_{n+1} - P_n}{T_{n+1} - T_n})$ (applied to the data shown in Figs. S6–S9) where P_n is the polarization value at T_n , P_{n-1} is the polarization value at a lower temperature T_{n-1} , and P_{n+1} is the polarization value at a higher temperature T_{n+1} [20]. For the estimations, density of the P(VDF-TrFE) was used as 1.77 g/cm^3 [21] and the value obtained from Archimedes method was used for the density of the BCST fillers. For the specific heat, 2000 $\text{J}/\text{kg}\cdot\text{K}$ and 500 $\text{J}/\text{kg}\cdot\text{K}$ were used for the pristine copolymer [22] and BCST particle [23], respectively. Using the rule of mixtures, 1784, 1681, 1585 $\text{J}/\text{kg}\cdot\text{K}$ was estimated for 5, 7.5 and 10 vol % BCST containing composites.

3. Results and discussion

In Fig. 1, x-ray diffraction (XRD) patterns of ceramic filler powder, pristine polymer and three composites are shown in the main panel. BCST shows pure perovskite peaks and P(VDF-TrFE) has a broad reflection around 19.2 $^\circ$ which corresponds to its polar phase. All composites include reflections from both the polymer and the ceramic filler. In the right panel, characteristic peak around 19.2 $^\circ$ of the polar β -phase of P(VDF-TrFE) is plotted separately.

Average particle size of the ceramic filler particles, checked by Dynamic Light Scattering (DLS) was obtained around 150 nm (Fig. 2(e)). In order to check the dispersion of the nanoparticles in the matrix, surface Scanning Electron Microscopy (SEM) images were captured. Surface SEM micrographs of the pristine copolymer and all composites in Fig. 2 show homogeneous distribution of the nanoparticles over the matrix volume for all composites. No significant agglomeration of the particles was observed. Cross-sectional SEM images show that the samples have

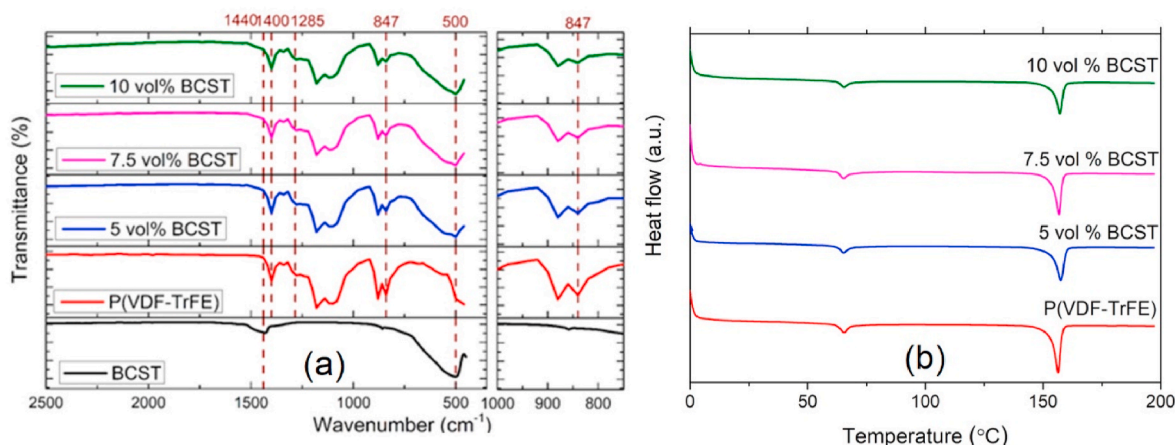


Fig. 3. (a) FTIR spectra of the BCST, pristine P(VDF-TrFE), and the composites, (b) DSC curves of pristine P(VDF-TrFE), and the composites.

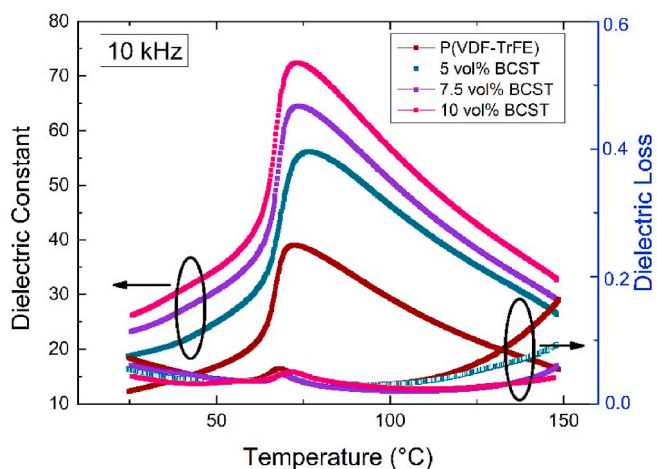


Fig. 4. Temperature dependence of the dielectric constant and dielectric loss of all samples measured at 10 kHz.

average thickness values in the range of 21–28 μm (Fig. 2(f) and S1–S3).

The interface between the particles and surrounding matrix is critical for the performance the resulting composite material. The interaction between the particles and the matrix polymer is examined by vibrational

spectroscopy. Fig. 3(a) presents the FTIR spectra of the pristine P(VDF-TrFE), BCST, and the composites. The signals of the ceramic particles and the pristine polymer are present in the spectra of the composites. No additional signal regarding the interaction of the particles and polymer was detected. Moreover, shifting of the polymer signals was not observed in the spectra of the composites, i.e. in the presence of the particles. The composites were subjected to thermal analysis using Differential Scanning Calorimetry (DSC). Pristine polymer shows melting temperature at 155 $^{\circ}\text{C}$ as shown in Fig. 3(b). This temperature remains unchanged upon incorporation of the particles even at high level of loading. Based on both FTIR and DSC results, one can claim that the particles were found to be inert against the matrix chains and no remarkable interaction between the particle and matrix polymer was detected.

Prior to adding BCST particles to form the composites, to check whether the BCST particles show the expected dielectric properties, sintered pellets were measured. In Fig. S4, temperature dependent dielectric constant and loss of BCST ceramic is shown, confirming the expected behaviour including a Curie temperature close to that of P(VDF-TrFE). We note that there will be differences due to the size effect between the dielectric properties of the ceramic nanoparticles used in the nanocomposites and the ceramic BCST pellet with micron-sized grains (SEM images not shown). In Fig. 4, temperature dependent dielectric constant and loss of all samples are shown at 10 kHz. Dielectric constant of the pristine polymer increases with increasing filler concentration, doubling for example for 10 vol % filler containing

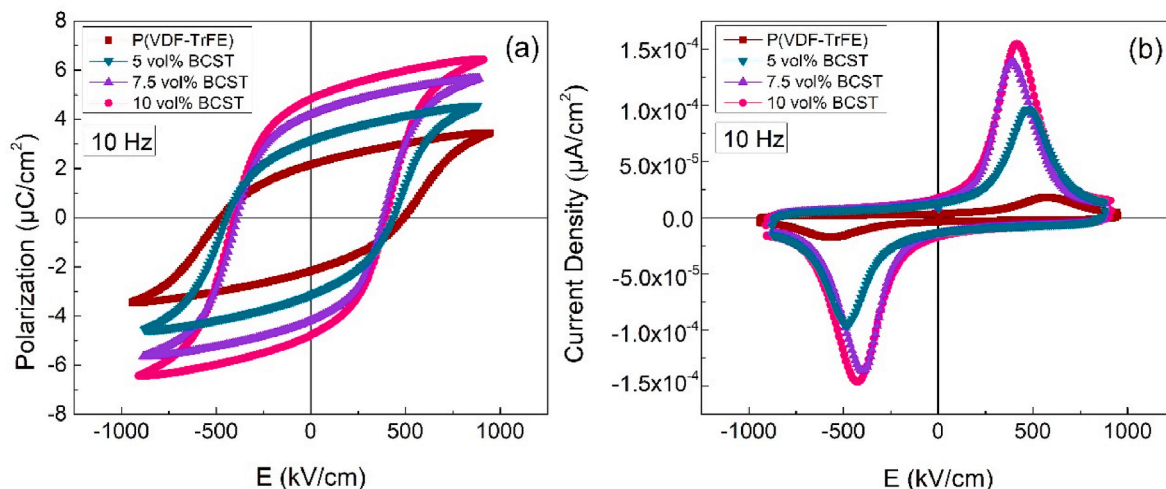


Fig. 5. (a) P(E) hysteresis loops and (b) the corresponding current-voltage curves of all samples at RT.

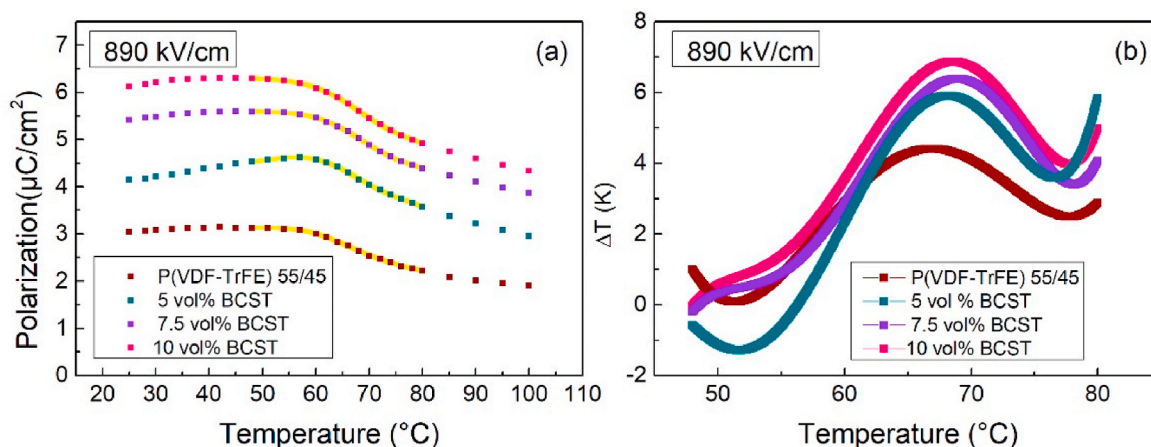


Fig. 6. (a) P(T) curves extracted from temperature dependent P(E) loops at 890 kV/cm, (b) ΔT vs T for all samples calculated using the indirect method at 890 kV/cm. Yellow solid lines in (a) show the polynomial fits to the P(T) data in the temperature range between 50 and 80 $^{\circ}\text{C}$ as depicted in the Experimental section. (For interpretation of the references to colour in this figure legend, the reader is referred to the Web version of this article.)

composite, compared to the pristine one. In all samples, clear anomalies in the dielectric constant and loss corresponding to the phase transition from ferroelectric to paraelectric phases are observed, defining the Curie temperature. No trend was observed in the change of Curie temperature with ceramics filler concentration. Dielectric loss increases with increasing temperature especially after 100 $^{\circ}\text{C}$. This increase is suppressed progressively by the increasing ceramic filler content. In pristine polymer, as well as for all composites, dielectric constant peak does not shift to higher temperatures when the frequency is changed, ruling out any relaxor ferroelectric behaviour (Fig. S5).

In Fig. 5, ferroelectric hysteresis loops and corresponding current density curves of all samples are shown. Both remanent and maximum polarization increases while coercive field decreases with the increasing filler concentration. Current density curves also show higher switching currents with increasing filler concentration, reflecting the increase in the polarization with increasing filler concentration.

In order to calculate the electrocaloric temperature change, hysteresis loops were measured as a function of temperature with small increments. For all samples, hysteresis loops at selected temperatures, P(T) curves derived from the hysteresis loops and ΔT of the samples estimated using the indirect method at different electric fields are included in Figs. S6–S9. In Fig. 6(a), P(T) curves for all samples are plotted at the largest electric field that could be applied, 900 kV/cm. It can be observed that just above the Curie temperature, P(T) decreases more quickly towards the paraelectric phase (i.e. $\frac{dP}{dT}$ becomes larger) as the filler content increases. This is reflected in the calculated ΔT values by the modified Maxwell's equations as shown in Fig. 6(b). ΔT increases as the ceramic filler content increases in the composites and 10 vol % filler containing composite shows the largest ΔT : 6.96 K under 900 kV/cm. We note that the negative electrocaloric effect that is observed in 5 vol % BCST containing sample between 25 and ≈ 55 $^{\circ}\text{C}$ is related to the slightly unsaturated loops obtained for this sample. As the temperature increases, coercive field decreases, and the loops reach full saturation and further increase of the temperature causes a decrease in the polarization as expected at and above the Curie temperature. The slight deviation from full saturation must have originated from the lower electric field that could be applied to this sample (Fig. 5(a)) compared to the pristine copolymer. This kind of artificial negative electrocaloric effect is common when the applied electric field is not enough to fully saturate the electrical polarization [24].

It is established that the improvement in the electrical properties of the nanocomposites is mainly due to the interface effect as outlined in the introduction section. Applied electric field polarizes the ceramic particles and as a result causes the formation of a local electric field

which amplifies the electric field at the interface, effectively increasing the polarization of the polymer composite under the same electric field. Interface effect explains the increase of the remanent and maximum polarization and apparent decrease of coercive field with the increasing filler content. In addition to the interface effect, increase in the crystallinity of the polymer upon ceramic filler addition has also been reported to contribute to the increase in the polarization and ΔT [11]. In our case, normalized DSC curves of the pristine copolymer and its nanocomposites (Fig. 3(b)) show lower heat of melting with increasing filler concentration, ruling out any crystallinity contribution to the electrocaloric effect.

In Table 1, ΔT and $\Delta T/\Delta E$ (electrocaloric temperature change obtained per unit applied field) of terpolymer and copolymer-based composites are compared with the literature. While terpolymer-based composites have larger ΔT and $\Delta T/\Delta E$ values in general, our copolymer-based composites also show superior electrocaloric performance compared to the pristine copolymer and terpolymer [15] and to one of the two other copolymer-based studies [7]. This is probably due to the large interface effect caused by the well-dispersed nanoparticles in the polymer matrix. The morphology of the particles is known to affect the interfacial area and boost the interface effect when the aspect ratio is increased. In our case, relatively small size of our nanoparticles (150 nm) compared to some other studies (300 nm [11] and 180 nm [8] in two terpolymer-based composites) might be contributing to the improved properties.

Recent report of superior electrocaloric effect on a copolymer-based composite is based on indirect method utilizing so-called PUND (positive-up negative-down) measurements. Superior electrocaloric effect is ascribed to the well-dispersed ceramic particles with fewer pores due to use of the hot press in combination with tape casting [19]. Owing to the normal ferroelectric nature of the copolymer-based composites and well-saturated hysteresis loops, we have successfully estimated ΔT values easily with the indirect method, without the need for PUND measurements used for leaky samples [19]. We note that maximum ΔT we obtained can be increased further by increasing the electric field, provided that the dielectric breakdown strength of the composites can be improved. It is well-known that dielectric breakdown strength of ferroelectric polymer-based composites with ceramic fillers decreases with increasing ceramic filler concentration [8,10,25]. This decrease is due to the inhomogeneous electric field distribution in the composites as well as structural defects in the heterogeneous composites [10]. By increasing the aspect ratio of the ceramic filler [8] or by adding an electrically insulating third component [10], dielectric breakdown strength can be increased further.

Table 1

Comparison of the electrocaloric properties with the literature.

Material	ΔE (kV/ cm)	ΔT (K)	$\Delta T/\Delta E$ (Kmm/ kV)	Measurement Method/ Material Type	Ref.
P(VDF-TrFE-CFE) (59.4/33.4/7.2 mol %) 0.9 Pb(Mg _{1/3} Nb _{2/3} O ₃ -0.1PbTiO ₃ (37.5 wt%)	750	9.4	0.0125	Direct-Relaxor	[2]
P(VDF-TrFE-CFE) (62.3/29.9/7.8 mol %) - Ba _{0.67} Sr _{0.33} TiO ₃ (10 vol%)	750	9	0.012	Direct-Relaxor	[3]
P(VDF-TrFE) (52/48)- Ba _{0.75} Sr _{0.25} TiO ₃ (10 vol%, 26 wt%)	600	2.5	0.004	Indirect- Ferroelectric	[4]
P(VDF-TrFE-CFE) (62.5/29/8.5 mol%) - P(VDF-TrFE) (55/45) (10 vol%)	750	5	0.0066	Direct-Relaxor	[26]
P(VDF-TrFE-CFE) (61.3/30.5/8.2 mol %) - BaZr _{0.2} Ti _{0.8} O ₃ (5 vol%)	900	7.4	0.00986	Direct-Relaxor	[27]
P(VDF-TrFE-CFE) (62.3/29.9/7.8 mol %) - Boron Nitride- (Ba,Sr)TiO ₃	2000	35	0.0175	Direct-Relaxor	[10]
P(VDF-TrFE-CFE) (63.2/29.7/7.1 mol %) - BaTi _{0.89} Sn _{0.11} O ₃ (7.5 vol %)	1000	9.1	0.009	Indirect-Relaxor	[28]
P(VDF-TrFE-CFE) (62.3/29.9/7.5 mol %) - Ba _{0.67} Sr _{0.33} TiO ₃	1000	14	0.014	Direct-Relaxor	[5]
P(VDF-TrFE-CFE) (62.5/29/8.5 mol %) - ZrO ₂ (3 vol %)	1400	9.2	0.00657	Direct-Relaxor	[6]
P(VDF-TrFE-CFE) (59.3/33.6/7.2 mol %)	3070	12	0.0039	Direct-Relaxor	[7, 15]
P(VDF-TrFE) (55/45)	2090	12	0.00574	Indirect- Ferroelectric	[7]
P(VDF-TrFE) (55/45)- 0.3(Ba _{0.7} Ca _{0.3})TiO ₃ - 0.7Ba(Ti _{0.8} Zr _{0.2})O ₃	500	9.1	0.018	Indirect- Ferroelectric	[19]
P(VDF-TrFE) (52/48) - Ba _{0.75} Sr _{0.25} TiO ₃	600	2.5	0.0041	Indirect- Ferroelectric	[4]
P(VDF-TrFE) (55/45)	900	4.4	0.0048	Indirect- Ferroelectric	This work
P(VDF-TrFE)- (10 vol %) BCST	900	6.9	0.00773	Indirect- Ferroelectric	This work

4. Conclusions

We have studied the electrocaloric effect of P(VDF-TrFE) based nanocomposites with BCST fillers. We observed that both the dielectric constant and the electrical polarization of the P(VDF-TrFE) increases with increasing filler concentration. Normal ferroelectric behaviour and saturated hysteresis loops of the composites allowed easy estimation of the electrocaloric temperature change using the indirect method. ΔT of the polymer composites increased with increasing BCST particles. We attribute the improvements in the electrical properties to the electric field amplifying effect of the interface between P(VDF-TrFE) and well-dispersed BCST nanoparticles with relatively small particle size. 10 vol % BCST containing composites yielded maximum ΔT of 6.9 K under 900 kV/cm. This result shows that copolymer-based composites can also be promising for electrocaloric cooling applications albeit with further improvement.

Declaration of competing interest

The authors declare that they have no known competing financial interests or personal relationships that could have appeared to influence the work reported in this paper.

Acknowledgements

This work is supported IZTECH Scientific Research Funds with the project number BAP2019IYTE0249. We acknowledge IZTECH Center for Materials Research for the use of XRD and SEM instruments, Geothermal Energy Research and Application Center for the DSC and Biotechnology and Bioengineering Application and Research Center for the FTIR measurements. We also thank Ceren Aşkın and Prof. Ender Suvacı for the complementary XRD measurements.

Appendix A. Supplementary data

Supplementary data to this article can be found online at <https://doi.org/10.1016/j.ceramint.2022.09.275>.

References

- [1] M. Valant, Electrocaloric materials for future solid-state refrigeration technologies, *Prog. Mater. Sci.* 57 (2012) 980–1009, <https://doi.org/10.1016/j.pmatsci.2012.02.001>.
- [2] S. Lu, Q. Zhang, Electrocaloric materials for solid-state refrigeration, *Adv. Mater.* 21 (2009) 1983–1987, <https://doi.org/10.1002/adma.200802902>.
- [3] R.J. Ma, Z.Y. Zhang, K.W. Tong, D. Huber, R. Kornbluh, Y.S. Ju, Q.B. Pei, Highly efficient electrocaloric cooling with electrostatic actuation, *Science* 357 (2017) 1130–1134, <https://doi.org/10.1126/science.aan5980>.
- [4] Y. Meng, Z.Y. Zhang, H.X. Wu, R.Y. Wu, J.H. Wu, H.L. Wang, Q.B. Pei, A cascade electrocaloric cooling device for large temperature lift, *Nat. Energy* 5 (2020) 996–1002, <https://doi.org/10.1038/s41560-020-00715-3>.
- [5] X.S. Qian, D.L. Han, L.R. Zheng, J. Chen, M. Tyagi, Q. Li, F.H. Du, S.Y. Zheng, X. Y. Huang, S.H. Zhang, J.Y. Shi, H.B. Huang, X.M. Shi, J.P. Chen, H.C. Qin, J. Bernholc, X. Chen, L.Q. Chen, L. Hong, Q.M. Zhang, High-entropy polymer produces a giant electrocaloric effect at low fields, *Nature* 600 (2021) 664–669, <https://doi.org/10.1038/s41586-021-04189-5>.
- [6] H.L. Hu, F. Zhang, S.B. Luo, J.L. Yue, C.H. Wang, Electrocaloric effect in relaxor ferroelectric polymer nanocomposites for solid-state cooling, *J Mater Chem A Mater* 8 (2020) 16814–16830, <https://doi.org/10.1039/d0ta04465b>.
- [7] Z.Y. Jiang, X.C. Zheng, G.P. Zheng, The enhanced electrocaloric effect in P(VDF-TrFE) copolymer with barium strontium titanate nano-fillers synthesized via an effective hydrothermal method, *RSC Adv.* 5 (2015) 61946–61954, <https://doi.org/10.1039/c5ra10508k>.
- [8] G.Z. Zhang, X.S. Zhang, T.N. Yang, Q. Li, L.Q. Chen, S.L. Jiang, Q. Wang, Colossal room-temperature electrocaloric effect in ferroelectric polymer nanocomposites using nanostructured barium strontium titanates, *ACS Nano* 9 (2015) 7164–7174, <https://doi.org/10.1021/acsnano.5b03371>.
- [9] J.F. Qian, R.C. Peng, Z.H. Shen, J.Y. Jiang, F. Xue, T.N. Yang, L.Q. Chen, Y. Shen, Interfacial coupling boosts giant electrocaloric effects in relaxor polymer nanocomposites: in situ characterization and phase-field simulation, *Adv. Mater.* 31 (2019), 1801949, <https://doi.org/10.1002/adma.201801949>.
- [10] G.Z. Zhang, B.Y. Fan, P. Zhao, Z.Y. Hu, Y. Liu, F.H. Liu, S.L. Jiang, S.L. Zhang, H. L. Li, Q. Wang, Ferroelectric polymer nanocomposites with complementary nanostructured fillers for electrocaloric cooling with high power density and great efficiency, *ACS Appl. Energy Mater.* 1 (2018) 1344–1354, <https://doi.org/10.1021/acsaem.8b00052>.
- [11] Q. Li, G.Z. Zhang, X.S. Zhang, S.L. Jiang, Y.K. Zeng, Q. Wang, Relaxor ferroelectric-based electrocaloric polymer nanocomposites with a broad operating temperature range and high cooling energy, *Adv. Mater.* 27 (2015) 2236–2241, <https://doi.org/10.1002/adma.201405495>.
- [12] X.Z. Chen, X.Y. Li, X.S. Qian, M.R. Lin, S. Wu, Q.D. Shen, Q.M. Zhang, A nanocomposite approach to tailor electrocaloric effect in ferroelectric polymer, *Polymer (Guildf.)* 54 (2013) 5299–5302, <https://doi.org/10.1016/j.polymer.2013.07.052>.
- [13] G.Z. Zhang, Q. Li, H.M. Gu, S.L. Jiang, K. Han, M.R. Gadinski, M.A. Haque, Q. M. Zhang, Q. Wang, Ferroelectric polymer nanocomposites for room-temperature electrocaloric refrigeration, *Adv. Mater.* 27 (2015) 1450–1454, <https://doi.org/10.1002/adma.201404591>.
- [14] F. le Goupil, K. Kallitsis, S. Tencé-Girault, N. Pouriamanesh, C. Brochon, E. Cloutet, T. Soulestin, F. Domingue Dos Santos, N. Stingelin, G. Hadziioannou, Enhanced electrocaloric response of vinylidene fluoride-based polymers via one-step molecular engineering, *Adv. Funct. Mater.* 31 (2021), 2007043, <https://doi.org/10.1002/adfm.202007043>.
- [15] B. Neese, B.J. Chu, S.G. Lu, Y. Wang, E. Furman, Q.M. Zhang, Large electrocaloric effect in ferroelectric polymers near room temperature, *Science* 321 (2008) (1979) 821–823, <https://doi.org/10.1126/science.1159655>.

- [16] D.A. Jesson, J.F. Watts, The interface and interphase in polymer matrix composites: effect on mechanical properties and methods for identification, *Polym. Rev.* 52 (2012) 321–354, <https://doi.org/10.1080/15583724.2012.710288>.
- [17] S.G. Lu, B. Rožič, Q.M. Zhang, Z. Kutnjak, R. Pirc, M. Lin, X. Li, L. Gorny, Comparison of directly and indirectly measured electrocaloric effect in relaxor ferroelectric polymers, *Appl. Phys. Lett.* 97 (2010), 202901, <https://doi.org/10.1063/1.3514255>.
- [18] Z.-Y. Jiang, G.-P. Zheng, X.-C. Zheng, H. Wang, Exceptionally high negative electro-caloric effects of poly(VDF-co-TrFE) based nanocomposites tuned by the geometries of barium titanate nanofillers, *Polymers* 9 (2017) 315, <https://doi.org/10.3390/polym9080315>.
- [19] T. Kawai, K. Kakimoto, Large electrocaloric effect of BCTZ/P(VDF-TrFE) 0-3 composites, *Mater. Lett.* 301 (2021), 130277, <https://doi.org/10.1016/j.matlet.2021.130277>.
- [20] F. le Goupil, A. Berenov, A.-K. Axelsson, M. Valant, N.M. Alford, Direct and indirect electrocaloric measurements on $\langle 001 \rangle$ -PbMg_{1/3}Nb_{2/3}O₃-30PbTiO₃ single crystals, *J. Appl. Phys.* 111 (2012), 124109, <https://doi.org/10.1063/1.4730338>.
- [21] H. Liu, X. Yang, Theoretical prediction of electrocaloric effect based on non-linear behaviors of dielectric permittivity under temperature and electric fields, *AIP Adv.* 5 (2015), 117134, <https://doi.org/10.1063/1.4936186>.
- [22] B.P. Neese, *Investigations of Structure-Property Relationships to Enhance the Multifunctional Properties of PVDF-Based Polymers*, The Pennsylvania State University, 2009.
- [23] A. Semenov, A. Dedyk, I. Mylnikov, O. Pakhomov, A. Es'kov, A. Anokhin, V. Krylov, A. Burovikhin, Y. Pavlova, A. Tselev, Mn-doped BaTiO₃ ceramics: thermal and electrical properties for multicaloric applications, *Materials* 12 (2019) 3592, <https://doi.org/10.3390/2Fma12213592>.
- [24] F. le Goupil, J. Bennett, A.-K. Axelsson, M. Valant, A. Berenov, A.J. Bell, T. P. Comyn, N.M. Alford, Electrocaloric enhancement near the morphotropic phase boundary in lead-free NBT-KBT ceramics, *Appl. Phys. Lett.* 107 (2015), 172903.
- [25] J.Y. Li, L. Zhang, S. Ducharme, Electric energy density of dielectric nanocomposites, *Appl. Phys. Lett.* 90 (2007), 132901.
- [26] X.Z. Chen, X.S. Qian, X.Y. Li, S.G. Lu, H.M. Gu, M.R. Lin, Q.D. Shen, Q.M. Zhang, Enhanced electrocaloric effect in poly(vinylidene fluoride-trifluoroethylene)-based terpolymer/copolymer blends, *Appl. Phys. Lett.* 100 (2012), 222902, <https://doi.org/10.1063/1.4722932>.
- [27] H. Aziguli, X. Chen, Y. Liu, G. Yang, P. Yu, Q. Wang, Enhanced electrocaloric effect in lead-free organic and inorganic relaxor ferroelectric composites near room temperature, *Appl. Phys. Lett.* 112 (2018), 193902, <https://doi.org/10.1063/1.5028459>.
- [28] Y.C. Lu, J.Y. Yu, J.Y. Huang, S.H. Yu, X.R. Zeng, R. Sun, C.P. Wong, Enhanced electrocaloric effect for refrigeration in lead-free polymer composite films with an optimal filler loading, *Appl. Phys. Lett.* 114 (2019), 233901, <https://doi.org/10.1063/1.5093968>.